



ELSEVIER

Available online at www.sciencedirect.com

SCIENCE @ DIRECT®

Surface & Coatings Technology xx (2004) xxx–xxx

**SURFACE
& COATINGS
TECHNOLOGY**

www.elsevier.com/locate/surfcoat

1

2 Large-area high-rate pulsed laser deposition of smooth $\text{TiC}_x\text{N}_{1-x}$ coatings 3 at room temperature—mechanical and tribological properties

4

J.M. Lackner^{a,*}, W. Waldhauser^a, R. Ebner^{a,b}

5

^aLaser Center Leoben, Joanneum Research Forschungsgesellschaft mbH, Leobner Strasse 94, A-8712 Niklasdorf, Austria

6

^bMaterials Center Leoben, Franz-Josef-Strasse 13, A-8700 Leoben, Austria

7

8 Abstract

9 Titanium carbonitride ($\text{TiC}_x\text{N}_{1-x}$) hard coatings possess excellent tribological behavior in metal punching and forming as well as high
10 biocompatibility. Because almost all PVD and CVD coating techniques for $\text{TiC}_x\text{N}_{1-x}$ coatings require substrate temperatures higher than
11 150–200 °C for reaching sufficient adhesion strength to the substrate surface, there is high demand in the development of large-area and high-
12 rate low-temperature vacuum deposition processes. In the present work, this call was fulfilled by the application of the room temperature
13 pulsed laser deposition (PLD) for $\text{TiC}_x\text{N}_{1-x}$ coating with various carbon (x) and nitrogen contents.

14 A pulsed Nd:YAG laser (wavelength: 1064 nm) was used for the vaporization of pure titanium targets in low-pressure $\text{N}_2/\text{C}_2\text{H}_2$
15 atmospheres. The highly ionized metal vapor was deposited onto polished substrates (molybdenum, AISI D2 steel), forming a nearly
16 particulate-free, very smooth and dense film structures, which can be hardly reached by using other PVD techniques. The variation of the gas
17 flow during deposition causes a change of the chemical composition and the microstructure of the nearly particulate-free coatings, and,
18 consequently, of the mechanical and tribological properties. The solid solution hardening of the fcc TiN lattice by low contents of carbon
19 increases the hardness and elastic modulus, while higher carbon contents decrease this effect. Furthermore, the maximum in hardness and
20 elastic modulus correspond with the minima in the friction coefficients (~0.2) and Wear rates of both the coated disc and the counterparts
21 (AISI 52100 (DIN 100Cr6) ball-bearing steel balls).

22 © 2004 Published by Elsevier B.V.

23 *Keywords:* Pulsed laser deposition; PLD; Laser ablation; Titanium carbonitride; TiCN; Tribology

24

25 1. Introduction

26 Over the past decade, the extension of the service life of
27 cutting and forming tools, and mechanical components has
28 been successfully achieved by applying thin hard coatings
29 onto their surfaces. Initially, titanium nitride (TiN) coatings,
30 favored for their high hardness as well as gold-like
31 appearance, were most widely used for Wear and corrosion
32 protection. Due to increasing demands on the surfaces of
33 tools and mechanical components, TiN coatings were
34 superseded by multi-component, multilayered and/or graded
35 coating materials like, e.g. titanium carbonitride ($\text{TiC}_x\text{N}_{1-x}$)
36 [1,2]. Ertuerk et al. [3] pointed out that $\text{TiC}_x\text{N}_{1-x}$ films are

solid solutions of fcc TiN and fcc TiC incorporating the 37
advantages and characteristics of both. In contrast to TiN, 38
 $\text{TiC}_x\text{N}_{1-x}$ coatings predominate with their better anti- 39
adhesive [4] and anti-abrasive [5,6] capability. 40

In recent years, methods based on moderate-temperature 41
CVD processes [7,8] and PVD processes [7,9,10] have been 42
developed allowing the production of hard coatings with 43
improved Wear resistance on temperature-sensitive materi- 44
als like tempered tool steels. Although the plastics industry 45
call for very low-temperature (<50 °C) vacuum coating 46
techniques, which distinguish by excellent adhesion to the 47
substrate surfaces towards chemical or galvanic coating, the 48
development of such techniques turned out to be very hard. 49
Additional difficulty is caused by particulates (droplets) 50
which result from the target evaporation in many PVD 51
processes (arc, sputtering, etc.). Besides influences of the 52
substrates, thickness of the coatings, deposition sequences 53

* Corresponding author. Tel.: +43 3842 81260 2305; fax: +43 3842 81260 23010.

E-mail address: juergen.lackner@joanneum.at (J.M. Lackner).

54 (in multilayer or graded coatings) and the type of Wear, also
 55 the surface morphology of the coating strongly affects the
 56 tribological performance of $\text{TiC}_x\text{N}_{1-x}$ coatings [2].

57 Pulsed laser deposition (PLD) is one of the few coating
 58 techniques which fulfill the demands of both room-temper-
 59 ature deposition and very smooth coating surfaces [11–15].
 60 By the development of a PLD coater designed for industrial
 61 applications at Laser Center Leoben, Austria, the high-rate
 62 PLD of almost all known engineering materials in inert or
 63 reactive high-vacuum atmospheres is now possible on large-
 64 area sheet and three-dimensionally shaped substrates [11–
 65 15]. The current work summarizes for the first time the
 66 achievements in large-area PLD coating on the example of
 67 the structural, mechanical and tribological behavior of
 68 $\text{TiC}_x\text{N}_{1-x}$ coatings.

69 2. Experimental

70 2.1. Coating deposition

71 In the pulsed laser deposition (PLD) technique, a pulsed
 72 laser beam is focused onto a target in order to evaporate its
 73 surface layers under vacuum or low pressure gas conditions.
 74 In the current work, the ablation of the pure titanium (99.9%
 75 Ti) was performed by a pulsed Nd:YAG laser system, which
 76 provides four beams of 1064-nm wavelength with 0.6-J
 77 pulse energy and 10-ns pulse duration at a repetition rate of
 78 50 Hz [11–15]. The vaporized material, consisting of atoms,
 79 ions and atomic clusters, is then deposited on the polished
 80 AISI D2 tool steel discs of 62 HRC hardness and
 81 molybdenum sheet, ultrasonically cleaned in pure acetone
 82 and alcohol. The advantage of this technique is the
 83 possibility to deposit coatings of high chemical purity and
 84 high adhesion to various substrate materials at room
 85 temperature [11–15]. The high adhesion—the best adhesion

86 class HF1 on the 6-part scale for the DIN Rockwell
 87 indentation test—was also found for the $\text{TiC}_x\text{N}_{1-x}$ graded
 88 multilayer coatings, which were deposited in different C_2H_2 /
 89 N_2 gas mixtures after evacuation of the vacuum chamber to
 90 3×10^{-3} Pa by the pumping system consisting of a
 91 turbomolecular and a rotary vane pump. The thickness of
 92 all coatings was set to 1.5 μm and contains an about 0.5- μm
 93 adhesive Ti–TiN graded interface and an about 1.0- μm -thick
 94 $\text{TiC}_x\text{N}_{1-x}$ top layer deposited in the specified $\text{C}_2\text{H}_2/\text{N}_2$ gas
 95 mixtures. The multi-beam PLD approach, showed in Fig. 1,
 96 allowed large-area coating with low deviation ($\sim 5\%$) of the
 97 deposited coating thickness over the used deposition height
 98 of ~ 22 cm [11,12]. The given deposition rates in Fig. 1
 99 reveal the high-rate film growth.

2.2. Coating characterization

100
 101 The surface morphology of the coatings was investigated
 102 by scanning electron microscopy (SEM). This microscope is
 103 equipped with an energy dispersive spectroscopic analyzer
 104 (EDS) for chemical analysis. X-ray diffraction (XRD)
 105 investigations of $\text{TiC}_x\text{N}_{1-x}$ coatings on Mo substrates were
 106 performed on a Bruker AXS D8 Discover diffractometer in
 107 grazing incidence alignment using 1° incidence of the
 108 primary $\text{CuK}\alpha$ X-ray beam. For hardness testing, a Fish-
 109 erscope H100 nanoindenter was used. The maximum loads
 110 applied on the Vickers indenter were 10 mN. Ball-on-disc
 111 tests at a sliding speed of 10 cm s^{-1} were performed in the
 112 tribological characterization of the coatings on the coated D2
 113 tool steel substrates at room temperature, ambient relative
 114 humidity ($\sim 60\%$) and 2 and 10 N load using AISI 52100 (DIN
 115 100Cr6) ball-bearing steel balls of 6-mm diameter as
 116 counterparts. The coated discs as well as the balls were
 117 cleaned with pure acetone and alcohol prior to testing. Optical
 118 profilometry was applied for Wear track and surface rough-
 119 ness inspection as well as for calculating the Wear rates.

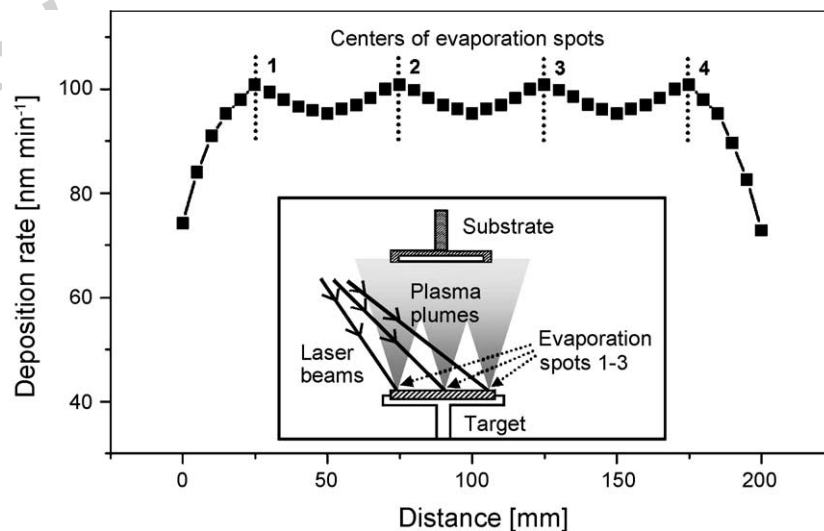


Fig. 1. Principle of the multi-beam pulsed laser deposition approach (insert) and deviation of the deposition rate of $\text{TiC}_x\text{N}_{1-x}$ (5 sccm C_2H_2 , 25 sccm N_2) over the deposited area.

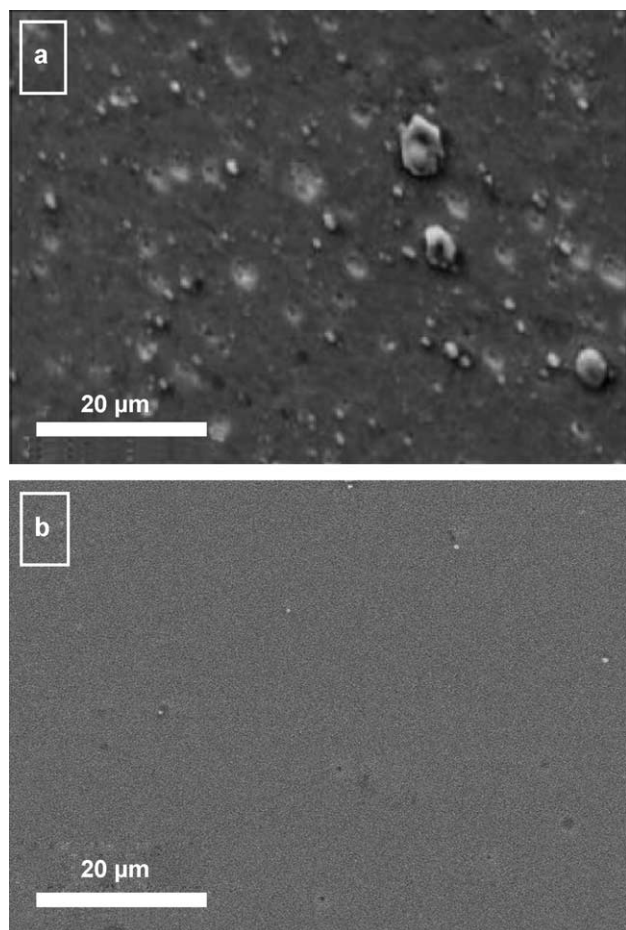


Fig. 2. Surface morphology of graded TiN–TiC_xN_{1-x} coatings found in SEM investigations: (a) unfiltered cathodic arc coating (3.2 μm thick, supplier: Ion Bond) [2], (b) PLD coating (1.5 μm thick).

3. Results and discussion

120

3.1. Coating morphology

121

In contrast to arc evaporated or magnetron sputtered TiC_xN_{1-x}, the PLD technique allows the deposition of very smooth and nearly particulate-free (droplet-free) hard coatings. This is shown in Fig. 2 by the comparison of a typical unfiltered cathodic arc film [2] and the PLD film. The particulates usually originate in the evaporation processes and are ejected besides the (partly) ionized vapor from the target [16]. In magnetron sputtering processes, these particulates are caused by chipping of either hard layers formed during sputtering of metallic targets with the reactive gas atmosphere (e.g. N₂, hydrocarbon compounds) or sintered grains from ceramic targets. In arc evaporated coatings, the particulates (droplets) originate from the push-out of molten target material at too high vapor pressures in the interaction zone of the arc and the target. Although both phenomena can also be found in pulsed laser ablation processes, the avoidance of particulates (droplets) is much easier for many target materials [17]. Besides the laser wavelength, the main influence on the droplet formation in PLD is the laser fluency on the target surface: A too high laser fluency results in high droplet density and rough coating surfaces, while a too low fluency (just higher than the evaporation threshold) prevents high-rate film growth and leads to inefficient deposition rates. Thus, the optimization process for the laser fluency is a golden mean between high-rate and high-quality film growth.

122

123

124

125

126

127

128

129

130

131

132

133

134

135

136

137

138

139

140

141

142

143

144

145

146

147

The average densities of particulates found on the arc and the PLD films were found to be about 22,000 and 800

148

149

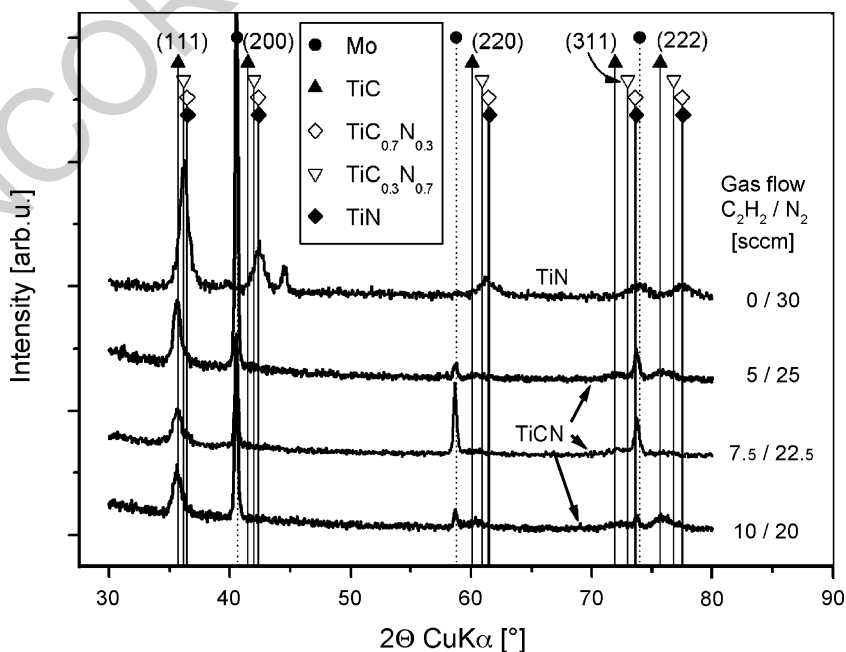


Fig. 3. XRD grazing incidence (1.0°) patterns of PLD TiC_xN_{1-x} and TiN coatings grown in atmospheres of various C₂H₂/N₂ gas flow mixtures on Mo substrates.

150 droplets per mm^2 coating surface and μm coating thickness,
 151 respectively. The average area covered with droplets is
 152 about $100\times$ higher for the arc ($\sim 60.4\%$) than for the PLD
 153 films (0.52%). Thus, the roughness was found to be about
 154 $28\times$ lower for the PLD ($R_a=4\text{ nm}$) than for the arc coating
 155 ($R_a=110\text{ nm}$).

3.2. Microstructure

156
 157 Due to the high energetic plasma, the microstructure of
 158 room-temperature PLD coatings [11–15] is mainly found to
 159 be of the Zone-T structure type of Thornton's structure zone
 160 model [18]. Such a structure was found too in the SEM

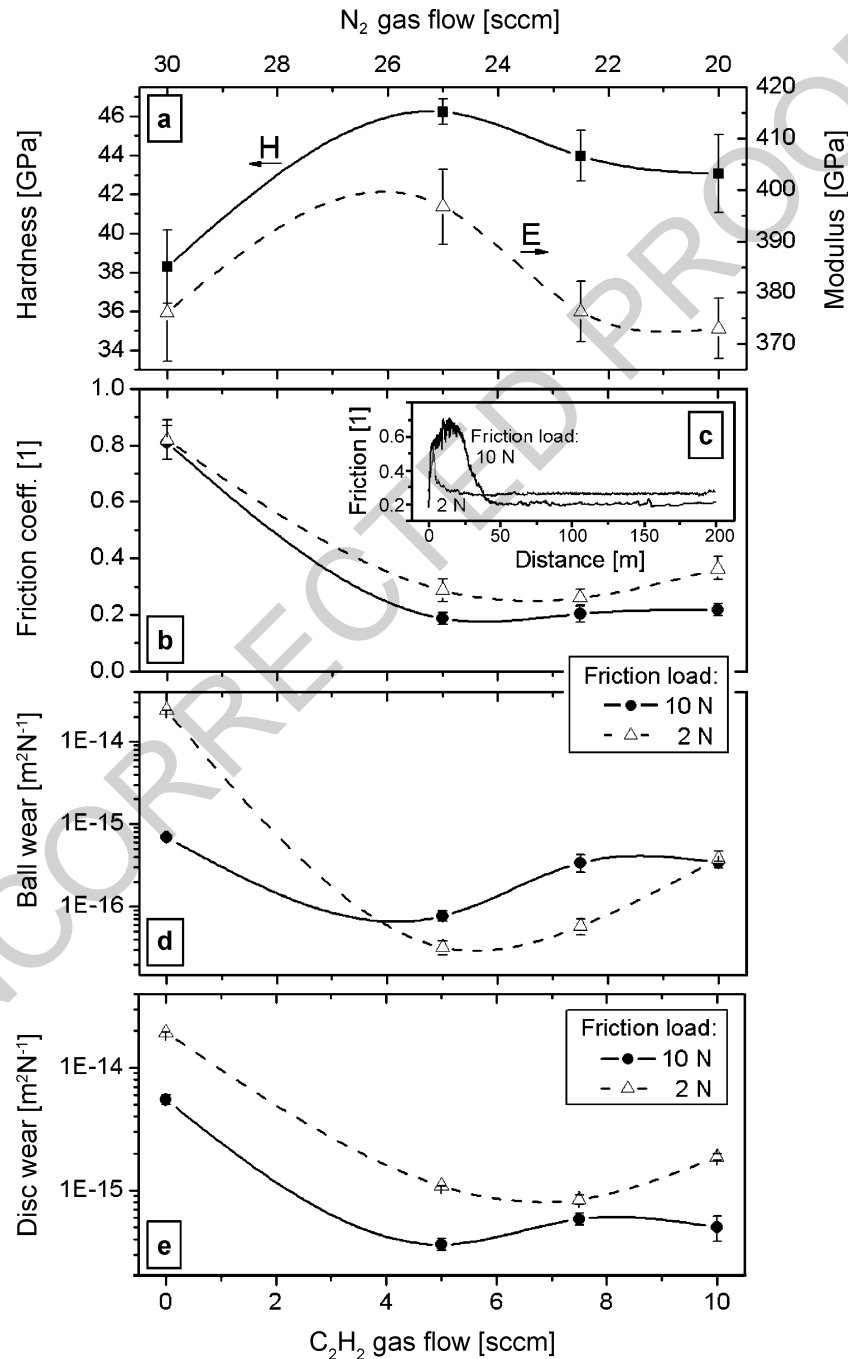


Fig. 4. Mechanical and tribological properties of the $\text{TiC}_x\text{N}_{1-x}$ (TiN) coatings in dependency on the C_2H_2 and N_2 gas flow during deposition: (a) Hardness and elastic moduli, (b) evolution of the friction coefficient during sliding at different friction loads (Deposition parameters of the coating: 5 sccm C_2H_2 , 25 sccm N_2 gas flow), (c) friction coefficient in the ball-on-disc tests, (d) wear rate of the uncoated AISI 52100 (DIN 100Cr6) ball counterpart, (e) wear rate of the $\text{TiC}_x\text{N}_{1-x}$ coated discs. (Tribological testing parameters: sliding distance: 200 m, sliding speed: 0.1 ms^{-1} , friction load: 2 and 10 N, temperature: $25\text{ }^\circ\text{C}$, relative humidity: $\sim 60\%$).

161 investigations of cross-sections of the $\text{TiC}_x\text{N}_{1-x}$ coatings.
 162 The microcrystalline structures grown at the low substrate
 163 temperatures are evident too in the broad peaks of the XRD
 164 patterns (Fig. 3), comparing TiN and $\text{TiC}_x\text{N}_{1-x}$ coatings
 165 deposited at various $\text{N}_2/\text{C}_2\text{H}_2$ gas mixtures. The change of
 166 the chemical composition of the coatings can be concluded
 167 from the increasing shift of the diffraction peaks to lower
 168 angles at higher C_2H_2 flows during deposition. This
 169 behavior is well known for $\text{TiC}_x\text{N}_{1-x}$ materials, which
 170 possess as well as pure TiN and TiC the NaCl-type fcc
 171 lattice structure [3]. Stress measurements, performed only
 172 for the pure TiN coating, revealed compressive stresses up
 173 to about -8 MPa [19], which cause the full peak shift for
 174 the TiN coatings from the position of unstressed TiN. Thus,
 175 it seems clear, that also a part of the shift to the lower
 176 diffraction angles of the $\text{TiC}_x\text{N}_{1-x}$ coatings is caused by
 177 compressive stresses. The crystallinity of the coatings,
 178 which are all (111) textured, seems to decrease with
 179 increasing C_2H_2 flows, possibly indicating the incorporation
 180 of hydrogen atoms during growth.

181 3.3. Mechanical and tribological behavior

182 The replacement of nitrogen atoms by carbon atoms
 183 leading to distortion of the fcc lattice results in the increase
 184 of hardness and elastic modulus of the coatings (Fig. 4a).
 185 Starting from pure TiN, low contents of carbon strengthen
 186 the lattice by solid solution hardening, while too high C
 187 contents (resulting from high C_2H_2 flows during deposition)
 188 result in a decrease of both mechanical properties. Possibly,
 189 the decrease of crystallinity affects the loss of hardness of
 190 these films.

191 The addition of carbon atoms to the TiN coating strongly
 192 influences the tribological behavior: As shown in Fig. 4b–e,
 193 the friction coefficients and Wear rates are drastically
 194 decreased in the $\text{TiC}_x\text{N}_{1-x}$ coatings of the higher hardness.
 195 A decrease of hardness increases the Wear rates again,
 196 found in the coatings deposited in atmospheres of higher
 197 C_2H_2 flows. The little higher disc Wear rates in the tests
 198 with 2 N friction load are mainly caused by the Wear
 199 calculation method of Holm, in which the Wear rates are
 200 defined as the proportion of lost volume to sliding distance
 201 and load [20]. In comparison to other low friction coatings
 202 like DLC, the same order of magnitude of the ball and disc
 203 Wear rates was found for the $\text{TiC}_x\text{N}_{1-x}$ coatings [21].
 204 Although the investigations have not been finished, the
 205 decrease in friction seems to be caused by the formation of
 206 carbon-rich transfer layers. Comparing the optical profilometry
 207 images of TiN and $\text{TiC}_x\text{N}_{1-x}$ (Fig. 5a and b), the
 208 sliding behavior of the AISI 52100 (DIN 100Cr6) ball-
 209 bearing steel ball is very different. While for TiN (Fig. 5a),
 210 rough Wear track surfaces are usually found, which are
 211 caused by the transfer of steel counterpart material to the
 212 TiN surface during Wear, the $\text{TiC}_x\text{N}_{1-x}$ Wear tracks are
 213 characterized by smooth grinding structures and the absence
 214 of asperities. On the counterparts to the $\text{TiC}_x\text{N}_{1-x}$ coatings,

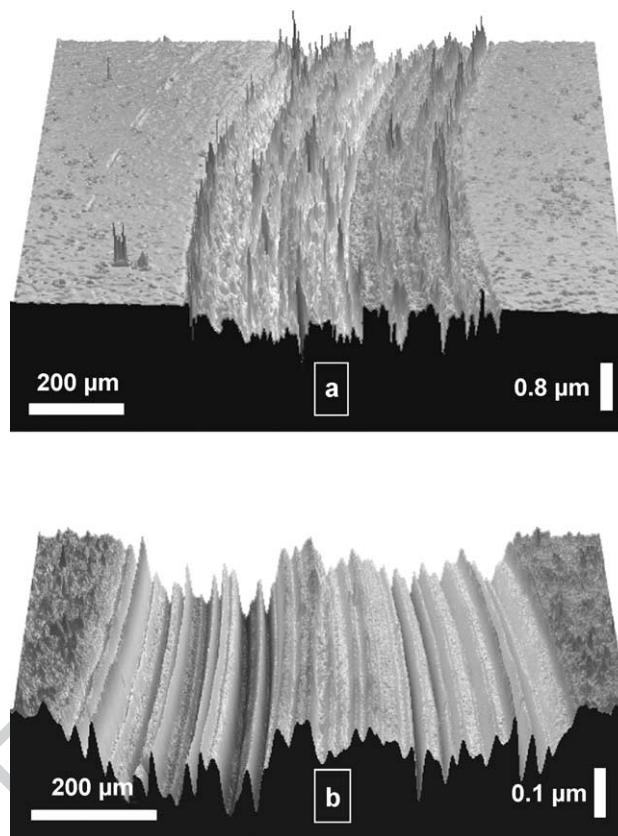


Fig. 5. Optical profilometry images of the wear tracks of (a) a TiN coating deposited at 30 sccm N_2 and (b) a $\text{TiC}_x\text{N}_{1-x}$ coating (5 sccm C_2N_2 , 25 N_2) sliding against uncoated AISI 52100 (DIN 100Cr6) pins at 10 N friction load. (Further tribological testing parameters: see description of Fig. 4).

215 thin transfer films consisting of mainly carbon and titanium
 216 atoms were found in EDS investigations. Thus, the low
 217 friction behavior of the PLD coatings seems to be caused by
 218 the missing of sticking of the steel counterpart material on
 219 the anti-adhesive $\text{TiC}_x\text{N}_{1-x}$ coating surfaces and, thus, the
 220 change from steel/steel transfer layer to carbon-rich transfer
 221 layer/ $\text{TiC}_x\text{N}_{1-x}$ coating contacts. Similar phenomena were
 222 found for $\text{TiC}_x\text{N}_{1-x}$ coatings deposited by other PVD and
 223 CVD techniques [2].

224 The friction coefficients were found to be lower for the
 225 lower friction force (2 N) applied in the ball-on-disc tests. The
 226 dependency of the friction coefficient on the sliding distance
 227 for a $\text{TiC}_x\text{N}_{1-x}$ sample in Fig. 4c reveals a further
 228 phenomenon: The run-in period is longer and reflected by
 229 higher friction coefficients for the higher friction load (10 N).
 230 This high friction during run-in (also for 2 N) confirms the
 231 absence of lubricant carbon layers, whose formation goes
 232 hand in hand with the decrease of the friction coefficient.
 233 Longer run-in sliding distances reveal a more difficult
 234 formation of the lubricant layers, which could be caused by
 235 the too high shear forces during the contact removing grown
 236 lubricant layers from the counterpart surface. The high
 237 friction coefficients result in high initial Wear of the coating
 238 and counterpart increasing the contact area [20]. As a reason,
 239 the Hertzian pressure and the shear forces decrease prevent-

240 ing the delamination of the lubricant carbon transfer layers
 241 from the coating and the counterpart. At the lower friction
 242 load (2 N), the same processes are running faster and the
 243 steady-state friction period is reached after shorter distances.
 244 The little higher friction coefficient at lower friction load
 245 reflects either the more difficult displacement of Wear debris
 246 out of the Wear track or the rougher surface of the Wear track
 247 found in the profilometry investigations.

248 4. Conclusions

249 The pulsed laser deposition (PLD) technique was applied
 250 in the current work for large-area and high-rate titanium
 251 carbonitride ($\text{TiC}_x\text{N}_{1-x}$) film growth on steel and molybde-
 252 num substrates at room temperature. The optimization of the
 253 laser fluency of the four Nd:YAG laser beams for titanium
 254 target ablation allows the growth of very smooth, nearly
 255 particulate-free (droplet-free) coatings in $\text{C}_2\text{H}_2/\text{N}_2$ gas
 256 mixtures. The variation of the $\text{C}_2\text{H}_2/\text{N}_2$ ratio resulted in
 257 significant changes of the microstructure, the mechanical
 258 and the tribological properties: While TiN coatings depos-
 259 ited in pure N_2 atmospheres possess high friction coef-
 260 ficients (~ 0.8) in the sliding contact of uncoated AISI 52100
 261 (DIN 100Cr6) counterparts due to the formation of steel
 262 transfer layers on the coated disc, the $\text{TiC}_x\text{N}_{1-x}$ coatings
 263 enable a drop of the friction coefficients to 0.2. The pin and
 264 disc Wear rates of $\text{TiC}_x\text{N}_{1-x}$ follow this drop, resulting in a
 265 reduction of both values to a 10th of the TiN/steel sliding
 266 pair. Furthermore, the hardness is influenced by the
 267 replacement of nitrogen by carbon atoms in the fcc lattice
 268 due to solid solution hardening. The variation of the friction
 269 load affects the run-in behavior of sliding due to load
 270 phenomena in lubricant transfer layer growth.

271 Acknowledgements

272 Financial support of this work by the Austrian Federal
 273 Ministry of Traffic, Innovation and Technology, the Austrian
 316

Industrial Research Promotion Fund (FFF), the Government
 of Styria, the Technologie Impulse Gesellschaft mbH in the
 frame of the Kplus programme and the European Union is
 highly acknowledged. 274
 275
 276
 277

References

- 278
 279
- [1] S.J. Bull, D.G. Bhat, M.H. Staia, Surf. Coat. Technol. 163–164 (2003) 280
 499–506. 281
- [2] S.J. Bull, D.G. Bhat, M.H. Staia, Surf. Coat. Technol. 163–164 (2003) 282
 507–514. 283
- [3] E. Ertuerk, O. Knotek, W. Bergmer, H.-G. Prengel, Surf. Coat. Technol. 284
 46 (1991) 39. 285
- [4] F.J. Teeter, in: Ceramic Coating, vol. 44, ASME, New York, 1993, 286
 p. 87. 287
- [5] E. Bergmann, H. Kaufmann, R. Schmid, J. Vogel, Surf. Coat. Technol. 288
 42 (1990) 237. 289
- [6] B. Navinsek, Mater. Manuf. Process. 7 (1992) 63. 290
- [7] W.D. Sproul, J. Vac. Sci. Technol. A12 (1994) 1595. 291
- [8] K. Narasimhan, S. Prasad, D. Bhat, Wear 188 (1995) 123. 292
- [9] J. Deng, M. Braun, Surf. Coat. Technol. 70 (1994) 49. 293
- [10] H.K. Tonshoff, C. Blawit, Surf. Coat. Technol. 93 (1997) 119. 294
- [11] J.M. Lackner, Innovative Coating by Pulsed Laser Deposition, PhD 295
 thesis, University of Leoben (Austria), 2003. 296
- [12] J.M. Lackner, W. Waldhauser, R. Ebner, C. Stotter, G. Jakopic, T. 297
 Schöberl, BHM 149 (2004) 118. 298
- [13] J.M. Lackner, W. Waldhauser, R. Ebner, J. Keckés, T. Schöberl, Surf. 299
 Coat. Technol. 177–178 (2004) 447. 300
- [14] J.M. Lackner, W. Waldhauser, R. Ebner, B. Major, T. Schöberl, Surf. 301
 Coat. Technol. 180–181 (2004) 585. 302
- [15] B. Major, W. Mroz, T. Wierzchon, W. Waldhauser, J.M. Lackner, R. 303
 Ebner, Surf. Coat. Technol. 180–181 (2004) 580. 304
- [16] B. Rother, J. Vetter, Plasma-Beschichtungsverfahren und Hartstoff- 305
 schichten, Dt. Verlag für Grundstoffindustrie, Leipzig, 1992. 306
- [17] D.B. Chrisey, G.K. Hubler, Pulsed Laser Deposition of Thin Films, 307
 Wiley, New York, 1994. 308
- [18] J.A. Thornton, J. Vac. Sci. Technol. 11 (1974) 666. 309
- [19] J.M. Lackner, W. Waldhauser, R. Ebner, B. Major, T. Schöberl, Thin 310
 Solid Films 181–181C (2003) 585. 311
- [20] K. Holmberg, A. Matthews, Coatings Tribology, Elsevier, Amster- 312
 dam, 1994. 313
- [21] J.M. Lackner, C. Stotter, W. Waldhauser, R. Ebner, W. Lenz, M. Beutl, 314
 Surf. Coat. Technol. 174–175 (2003) 402. 315